Available online at www.sciencedirect.com
ScienceDirect
Ceramics International 37 (2011) 3617–3625
CERAMICS INTERNATIONAL
www.elsevier.com/locate/ceramint

# Study of ceramic ultrafiltration membrane support based on phosphate industry subproduct: Application for the cuttlefish conditioning effluents treatment

Mouna Khemakhem, Sabeur Khemakhem, Salwa Ayedi, Raja Ben Amar *

*Laboratoire Sciences des Matériaux et Environnement, Université se Sfax, Faculté des sciences de Sfax, Rte. de Soukra Km 4, 3018 Sfax, Tunisia*

Received 18 May 2011; accepted 10 June 2011
Available online 17 June 2011

**Abstract**

The development and the characterisation of a new support for ultrafiltration membranes prepared from the mud of the hydro cyclone laundries of phosphate are presented. The choice of this material is based mostly on its low cost (considering its abundance in the Tunisian ores). Indeed, the use of this material for membrane preparation allows a good management of this subproduct which represents a major problem in phosphate transformation industry due to the resulting environmental pollution.

Paste from the mud of the hydro cyclone laundries of phosphate was extruded and heated at 900 °C to produce a porous tubular support having an average pore diameter and a porosity of about 1.05 μm and 39%, respectively. The properties regarding to mechanical and chemical resistances are very interesting. The deposition of the ultrafiltration layer from zirconium material was performed by slip-casting method. The heating treatment at 700 °C leads to an average pore size of 5 nm. The determination of the water permeability shows a value of 86 l/h $m^2$ bar. This membrane can be used for crossflow ultrafiltration. The application of the cuttlefish effluent treatment shows an important decrease of turbidity, inferior to 1.5 NTU and chemical organic demand (COD), retention rate of about 60%. So, it seems that this membrane is suitable to use for wastewater treatment.



*Keywords:* Mud of the hydrocyclone laundries of phosphate; Ceramic support; Ultrafiltration membrane; Cuttlefish effluents

## 1. Introduction

Due to their potential application in a wide range of industrial processes, membrane technologies have received an increasing interest. Ultrafiltration and microfiltration are often used to remove particles, microorganism, and colloidal materials from suspensions [1,2]. The use of ceramic membranes has many advantages such as high thermal and chemical stability [3–5], long lifetime, and physic-chemical inertia [1].

From a technical-economic point of view, new composite ceramic microfiltration (MF) and ultrafiltration (UF) membranes have been produced recently from abundant natural materials like clay [6] and phosphate [7] as well as from abundant subproduct resulting from some industrial transformation like fly ash obtained from coal fired power station [8].

In the phosphate industry transformation, we can notice the formation of huge quantities of subproduct resulting from the apatite washing step following by extraction. The solid waste is composed mostly of a very small particles based on a mixture of clay and apatite resulting in a significant product of mud whose stockage generate enormous environmental problems.

In the literature there is almost no previous works which treat the upgrade of the phosphate industry subproduct. We can noticed particularly works done by Imen Khiari, Islem Chaari and al. [9] whose have used the mud of the hydrocyclone laundries of phosphate to prepare porous material based on lightweight aggregates used as adsorbent to retain lead from heavy metal solutions.

Thanks to very small clay and apatite particles which composed this mud, the phosphoric subproduct can give also ceramic pastes of a good plasticity and an easy shaping. So, an

* Corresponding author. Tel.: +216 74 2 76 400; fax: +216 74 274 437.
*E-mail address:* raja.rekik@fss.rnu.tn (R.B. Amar).

0272-8842/$36.00 
doi:10.1016/j.ceramint.2011.06.020

adapted configuration for ceramic microfiltration or ultrafiltration membrane can be performed.

The aim of this work was to prepare a low cost porous ceramic composite membranes using abundant material based on the mud of the hydrocyclone laundries of phosphate. In the first part of this work we will present the conditions of the elaboration of the membrane tubular support using appropriate ceramic techniques. In the second part, the elaboration of ultrafiltration layer supported by the mud of the hydrocyclone support and their main properties will be discussed. The last part of this work concerns the application of the ultrafiltration elaborated membrane to the treatment of cuttlefish conditioning wastewater.

## 2. Materials and methods

### 2.1. Characterization of the mud of the hydrocyclone laundries of phosphate

The mud of the hydrocyclone laundries of Tunisian phosphate is coming from Gafsa in the south of Tunisia. It was obtained by the apatite washing step following by extraction process. Different techniques were used for the characterization.

The chemical composition of mud of the hydrocyclone laundries was determined by spectroscopic techniques, as X-ray fluorescence for metals and by atomic absorption for alkaline earth metals.

The powder morphology as well as the microstructure of samples was obtained using a HITASHI scanning electron microscope (SEM).

Purity of the powder was tested by IR spectral analysis. An IR transmittance spectrum of the ground sample was obtained in the 4000–400 $cm^{-1}$ range with a SHIMATZU IR 470 spectrometer.

Phases present in the powder compositions were analyzed using an X-ray diffractometer (Siemens, Germany) with Cu Kα radiation.

### 2.2. Elaboration of porous support

Ceramic membranes have generally a composite structure, composed at least of two layers: A macroporous one which constitutes the support and a thin active layer.

The elaboration of the ceramic support implies the following sequence of operations:

- preparation of a plastic ceramic paste;
- shaping by extrusion;
- consolidation by thermal treatment.

In Fig. 1, the process of the ceramic preparation was described.

The preparation of paste requires a specific ageing and also the use of organic additives to allow the powder dispersion and the adjustment of the paste rheological behaviour. These additives ensure a significant mechanical resistance before the final consolidation by sintering. The principal advantage of the organic additives is that they are eliminated by combustion during the thermal treatment.

The optimized composition of the paste is (values are given in wt%):

- Mud of hydro cyclone powder 82.4%.
- Methocel (The Dow Chemical Company): 4%.
- Amijel (Cplus 12076, Cerestar): 4%.
- Porosity agent: starch (RG 03408, Cerestar): 9.6%.

Before extrusion, an ageing stage of the paste is necessary to obtain a good homogeneity and the hydration of the cellulose

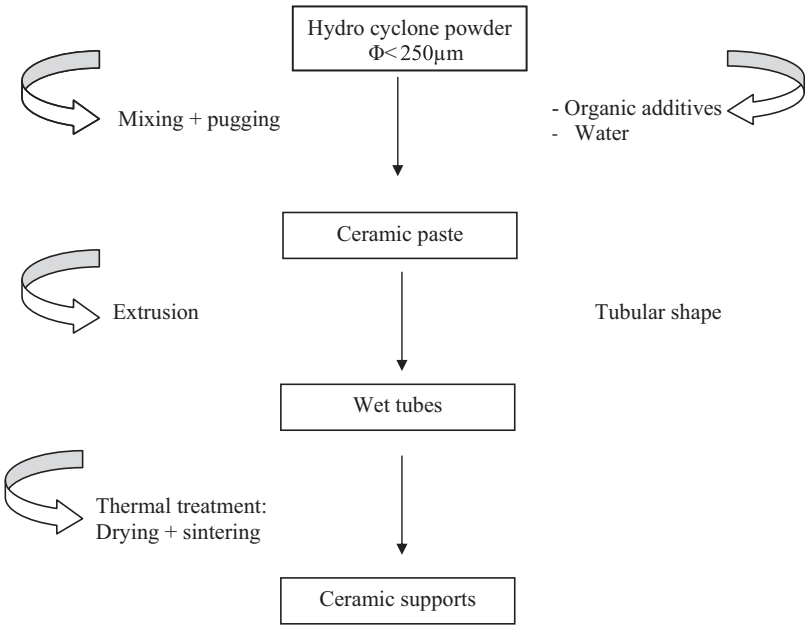


Fig. 1. Various steps of macroporous ceramic preparation.

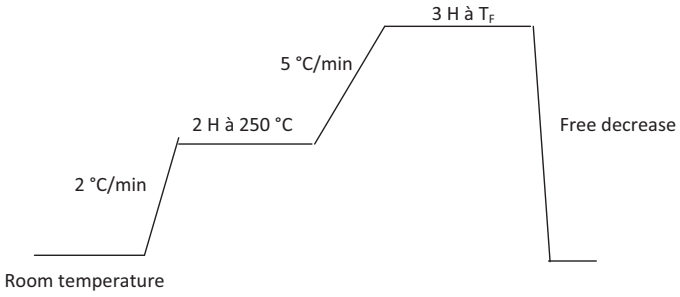


Fig. 2. Temperature–time schedule used.

binders. The time necessary for this stage is 24 h. Shaping was performed by extrusion. After that, the wet support was set on rollers to obtain a homogenous drying at room temperature. Finally, a thermal treatment was carried out in a programmable furnace at different final temperatures; the adapted firing treatment was established from the thermal analysis data (Fig. 2). Two steps have been determined: the first one for the elimination of organic additives at 250 °C (temperature was maintained for 2 h) and the second one for the sintering at different temperatures. The temperature–time schedule not only affects the pore diameters and porous volume of the final product but also allows obtaining the final morphology and mechanical strength. Sintering was performed at a temperature ranging from 800 °C to 1000 °C (Fig. 3).

### 2.3. Preparation of the zirconia ultrafiltration layer

The active ultrafiltration layer from zirconia powder (specific area of 42 $m^2$) was prepared by a slip-casting process [10] on mud of hydrocyclone powder support (closed-end tubes of 150 mm in length, with an inner diameter of 5 mm). The optimum composition which permits uniformity of the coating deposited on the inner surface of the macroporous support was done in Table 1.

### 2.4. Filtration pilot

Cross flow ultrafiltration tests were performed using a homemade pilot plant (Fig. 4) at a temperature of 25 °C and transmembrane pressure (TMP) range between 1 and 4 bar. The transmembrane pressure was controlled by an adjustable valve at the concentrate side. The flow rate was fixed at 1.76 m $s^{-1}$. Before the tests, the membrane had been conditioned by

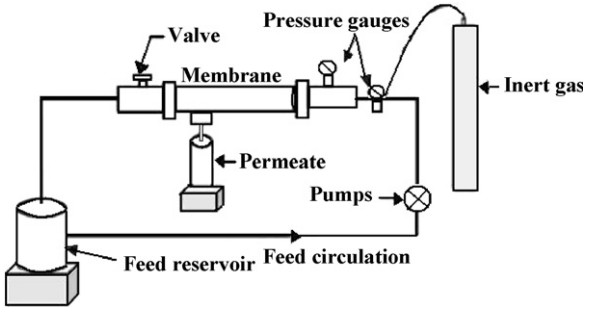


Fig. 3. Scheme of the pilot plant.

Table 1
Composition of the slip.

| Component | wt% |
|---|---|
| Water | 66 |
| Polyvinyl alcohol (PVA) (aqueous solution) | 30 |
| $ZrO_2$ | 4 |

immersion in pure deionised water for at least 24 h. The duration of each test ranged from 1 to 3 h. The water permeability of the membrane was giving by determining the variation of the distilled water permeate flux at different transmembrane pressure values. The regeneration of the membrane was carried out by firstly, back-flushing procedure for 15 min, then acidic (nitric acid 2% at 60 °C) and basic (NaOH 2% at 80 °C) solutions were alternatively circulated for 20 min.

## 3. Results and discussion

### 3.1. Characterisation of the mud of hydrocyclone powder

#### 3.1.1. Chemical composition

The chemical composition of the mud of hydro cyclone powder is shown in Table 2. It reveals that the major components were silica ($SiO_2$: 38.89%) and calcium oxide (CaO: 19.98%). The other percentage such as $P_2O_5$ (8.40%), $AL_2O_3$ (6.75%), $CO_2$ (6.06%) are also relatively high.

This phase composition is similar to that of the clay with a difference regarding the relatively high percentage of $P_2O_5$ [6].

#### 3.1.2. Thermal analysis

The TGA-DTA data of the mud of hydrocyclone powder is represented in Fig. 4. Two endothermic peaks were detected. The first peak with a significant intensity appears at 45.9 °C, due to a weight loss of 7.22% of the initial weight. It corresponds to the departure of water (moisture or adsorption) due to attraction on the surface of the sample and zeolitic water inserted between the layers or in the cavities of the crystalline structure [11]. The second peak with a less intensity appears at 665.22 °C, accompanied by a weight loss of 20.62% of the initial weight. It corresponds to the decomposition of carbonates [12].

#### 3.1.3. Phase identification

XRD data for the mud of hydrocyclone powder sample sintered at 900 °C are shown in Fig. 5. The major crystalline phases identified were quartz ($SiO_2$) and fluorine apatite (Fl). A minority of Ca: calcite, Sep: sepiolite, Ma: magnesite, K: kaolinite, Si: siderite, can be seen also on the spectrum.

#### 3.1.4. IR spectrum

The IR spectrum of the sample sintered at 900 °C is shown in Fig. 6. Recorded IR spectrum of the sample shows bands relative to mud of hydrocyclone laundries. The strongest peaks at 1030, 1090 and 964 $cm^{-1}$ are attributed to $PO_4^{3-}$ [13], the peaks at 566 and 600 $cm^{-1}$ are assigned to P–O mode [14]. 3518 $cm^{-1}$ band may come from lattice P–OH because this band exists in the range of 3550–3200 $cm^{-1}$ for hydrated $H_2O$.

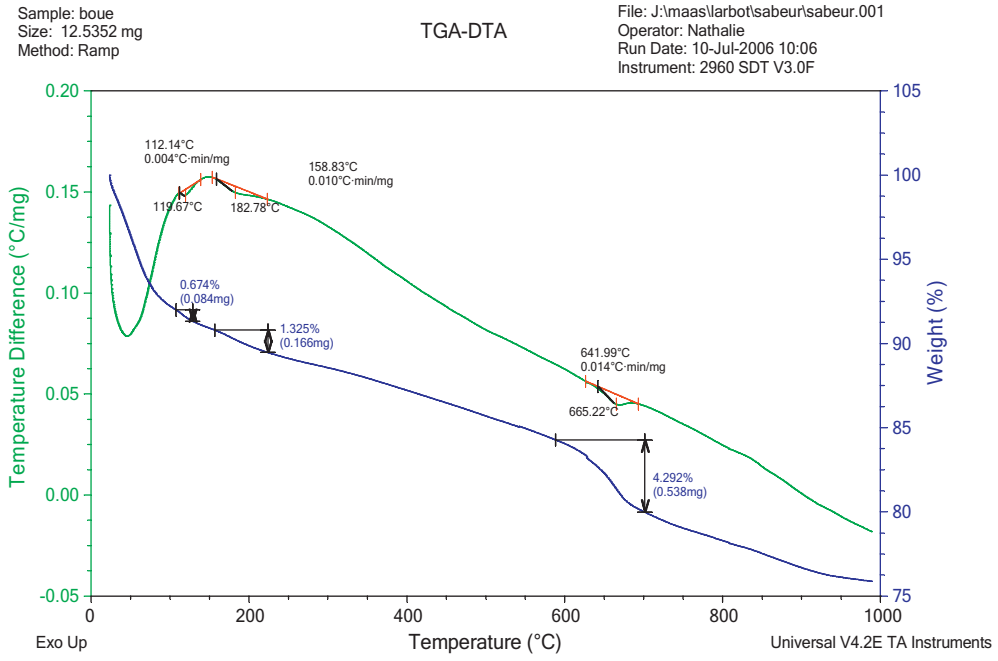


Fig. 4. TGA–DTA data of the hydrocyclone powder.

Table 2
Chemical analysis of the mud of the hydro cyclone laundries of phosphate powder.

| | Elements | | | | | | | | | | LOI* |
|---|---|---|---|---|---|---|---|---|---|---|---|
| | $P_2O_5$ | CaO | $SO_4$ | $SiO_2$ | $Fe_2O_3$ | $F^-$ | COT | $AL_2O_3$ | MgO | $CO_2$ | |
| wt% | 8.40 | 19.98 | 2.47 | 38.89 | 1.09 | 1.30 | 1.45 | 6.75 | 1.84 | 6.06 | 11.77 |

*Loss on ignition.

469 $cm^{-1}$ band results from the $\upsilon_2$ phosphate mode [15]. In addition, the bands relative to $CO_3^{2-}$ ions [16,17] are present at 870 and 1463 $cm^{-1}$.

### 3.1.5. Particle sizes distribution

Particle size determination of the mineral powder was made based on the principle of sedimentation, which aims to determine the distribution of powder particles.

Fig. 7 shows the results obtained as a cumulative curve. The crushed raw material has a major mixed grain size between 50 μm and 70 μm.

## 3.2. Characterisation of the support

For the development of high-quality supports, the following properties are of major importance: pore size distribution,

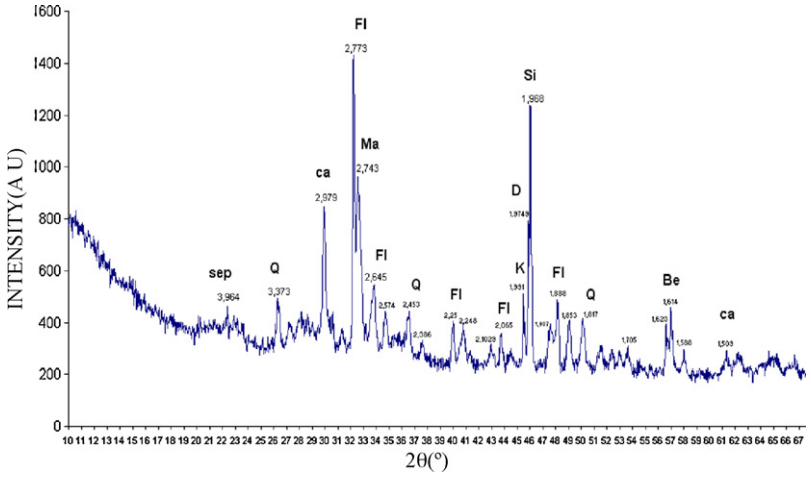


Fig. 5. X-ray diffractogram of the hydrocyclone powder sample: quartz (Q), fluorine apatite (Fl), Ca: calcite, Sep: sepiolite, Ma: magnesite, K: kaolinite, Si: siderite.

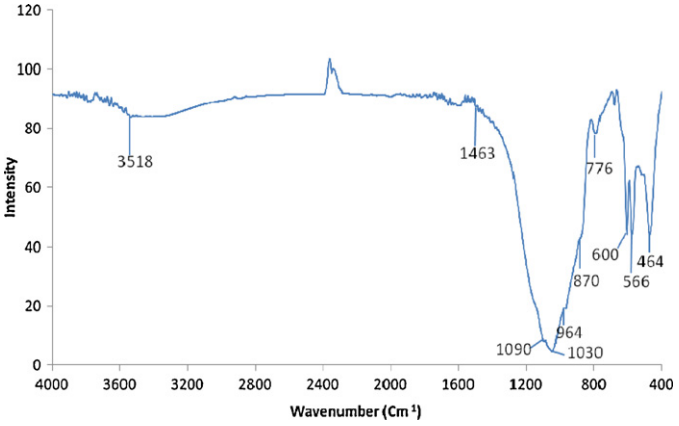


Fig. 6. IR spectrum of the hydrocyclone powder sample.

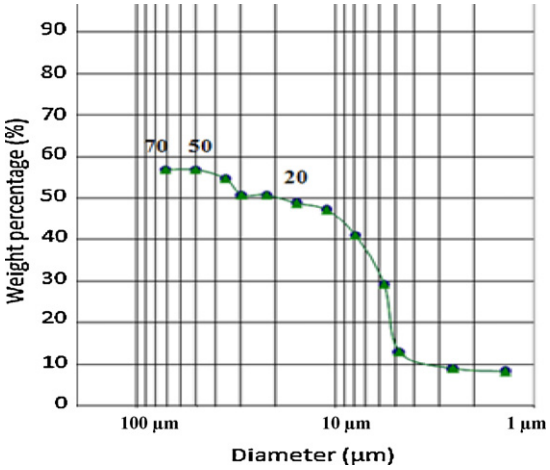


Fig. 7. Mud of hydrocyclone powder particle size distribution.

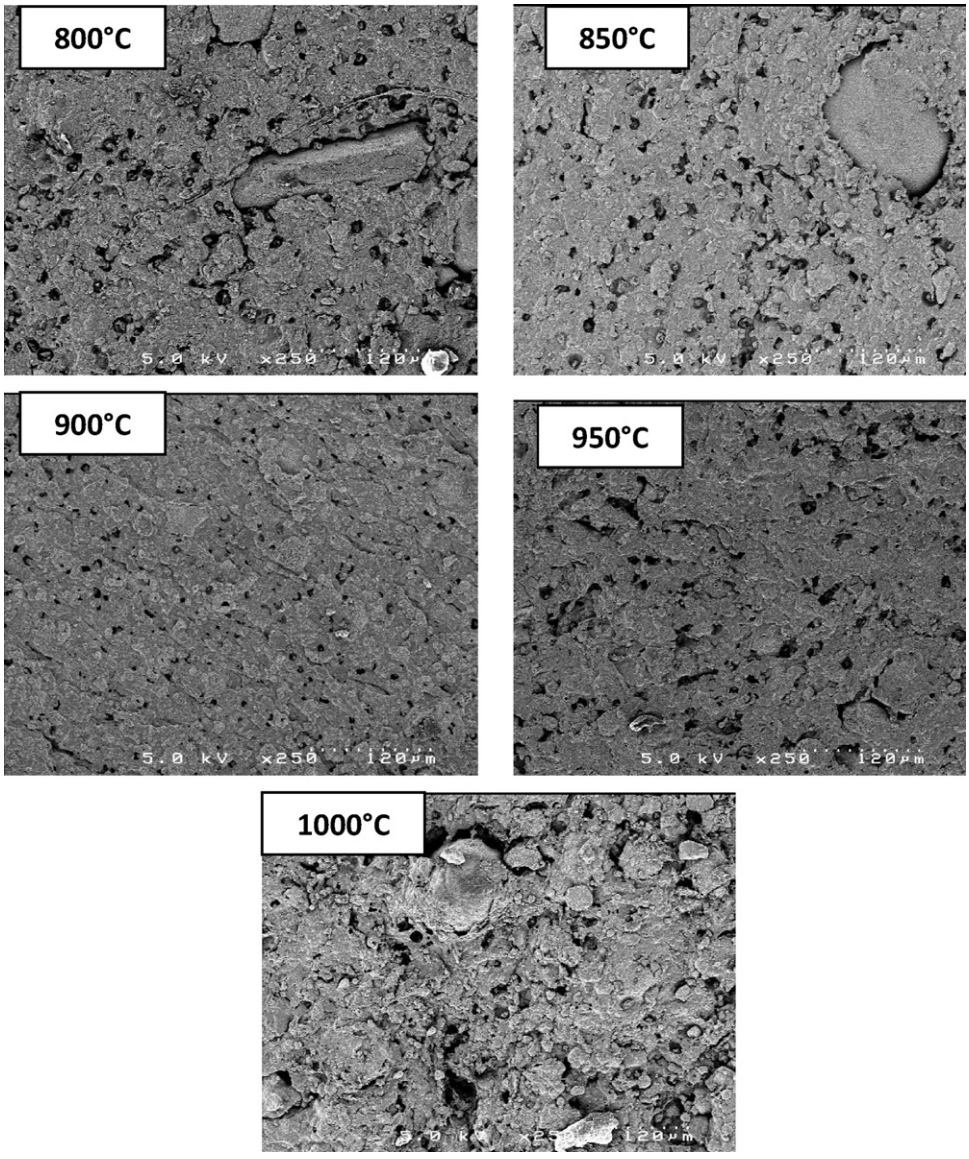


Fig. 8. Micrographs (SEM) of internal surface of tubular supports at various sintering temperatures.

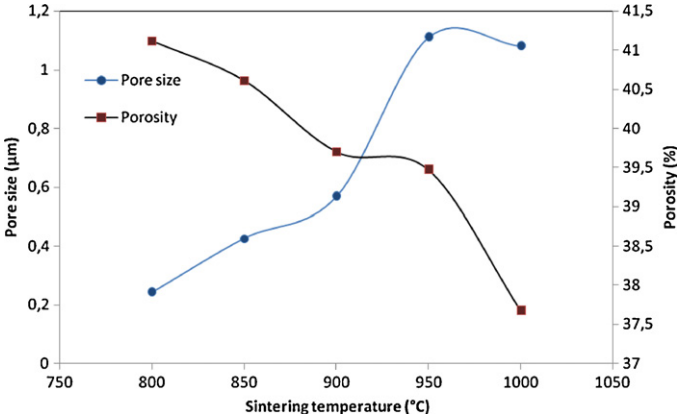


Fig. 9. Variation of pore diameter and pore volume with sintering temperature.

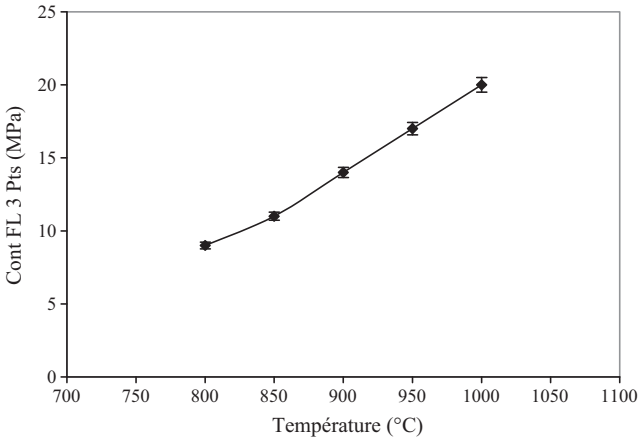


Fig. 11. Variation of tensile strength with sintering temperature of the support.

porosity, surface texture, mechanical properties and chemical stability.

### 3.2.1. Scanning electron microscopy (SEM)

The evolution of densification and surface quality of the support sintered at different temperatures were determined by scanning electron microscopy. The micrographs relating to the evolution of the microstructure of the mud of hydrocyclone membranes with the increasing sintering temperature (from 800 to 1000 °C) are shown in Fig. 8. The formation of particle boundaries was achieved within this narrow temperature range. The optimal sintering temperature was determined by comparing the texture of samples sintered at the different temperatures. At 900 °C, the support surface was homogeneous and did not present any macrodefects (cracks, etc.). A smooth inner surface was also observed which will allow the deposit of a homogeneous membrane layer.

### 3.3. Mercury porosimetry

The evolution of the support characteristics (pore diameter and porosity) with sintering temperature is shown in Fig. 9. The evolution of the average pore diameter and the porosity with the temperature of sintering reveals that the porosity decreases from 41 to 37% between 800 and 1100 °C, while the pore diameter increased from 0.25 to 1.08 µm. This behaviour corresponds to an opening of the pores at low temperature. The beginning of the material densification occurred when the temperature increases.

At 900 °C, the characteristics of the support are an average pore diameter of 1.05 µm and a porosity of 39% (Figs. 9 and 10).

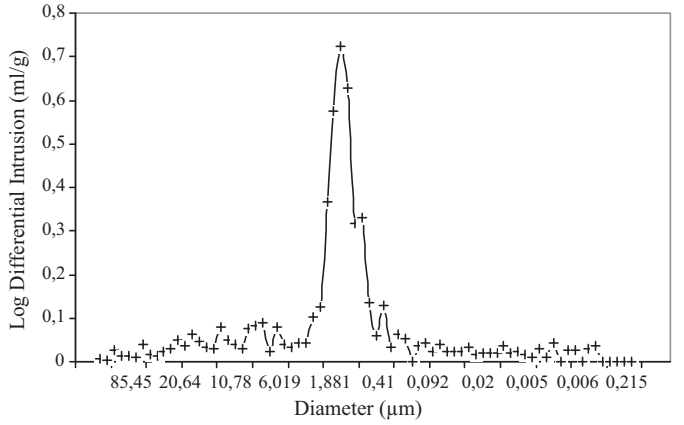


Fig. 10. Pore diameters of the mud of hydrocyclone supports.

### 3.4. Mechanical resistance

The mechanical resistance tests were performed using the three points bending method (LLOYD Instrument) to control the resistance of the support tube fired at different temperatures. Fig. 11 shows the variation of tensile strength with sintering. In accordance with the SEM pictures and the porosity values, the increase of the sintering temperature is accompanied with a densification phenomenon and consequently an increase in the tensile strength from 9.8 MPa at 800 °C to 22.9 MPa at 1000 °C.

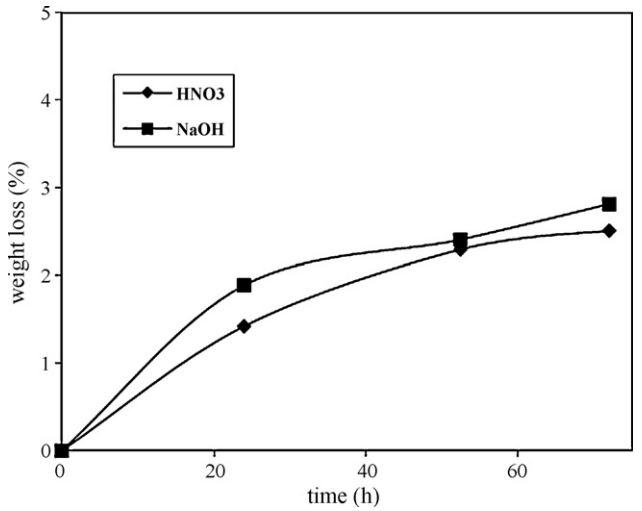


Fig. 12. Weight loss of support in nitric acid and soda solutions as a function of time.

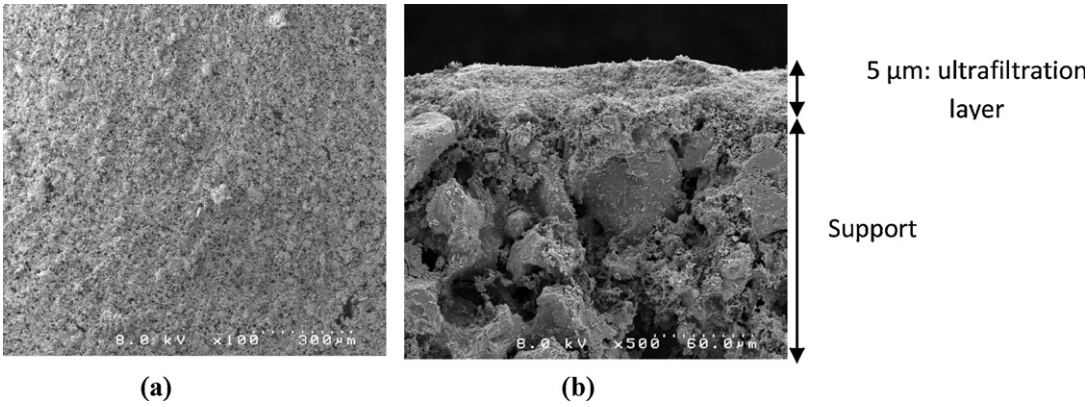


Fig. 13. Micrographs (SEM) of zirconia ultrafiltration layer: (a) general view of the surface; (b) cross-section view.

### 3.5. Chemical resistance

The results reported in Fig. 12 shows that mud of hydrocyclone support presents a chemical resistance towards the acid and basic solutions. In fact the weight loss is negligible when a sample was exposed during 72 h into a soda aqueous solution at a pH of 9 and did not exceed 3% when it is exposed to a nitric acid aqueous solution at a pH of 3 under the same conditions regarding time and temperature.

### 3.6. Characterisation of the ultrafiltration membrane

#### 3.6.1. Scanning electron microscopy (SEM)

The observation of the morphology and the surface quality of the thin layer of ultrafiltration by scanning electron microscopy (SEM) shows a quite homogeneous and a dense ceramics of well-closed surface with a good adhesion on the support. The layer thickness is about 5 µm (Fig. 13).

#### 3.6.2. Mercury porosimetry

The mean pore diameters determined by mercury porosimetry were centred near 5 nm for the deposited ultrafiltration layer (Fig. 14).

This result is very interesting since the UF active layer have been directly deposited on the support without the need of a second MF layer as it was usually considered [18,19]. This procedure will make it possible to limit the resistance against the mass transfer and consequently to increase the filtration performances.

#### 3.6.3. Determination of membrane permeability

The membrane permeability ($L_p$) can be determined using the variation of the distilled water flux ($J_w$) with the transmembrane pressure ($\Delta P$) following the Darcy's law:

$$J_w = L_p \Delta P, \quad \text{where } \Delta P = \left[\frac{(P_{inlet} + P_{outlet})}{2} - P_f\right]$$

where $P_{inlet}$ = inlet pressure; $P_{outlet}$ = outlet pressure; $P_f$ = filtrate pressure.

The permeability of the ultrafiltration membrane was determined from the values of fluxes measured after stabilization for each working pressure (after 45 min of water filtration). It can be seen that the water flux increases linearly with increasing the applied pressure (Fig. 15). The membrane permeability "$L_p$" was found to be equal to 86 l/h m$^2$ bar.

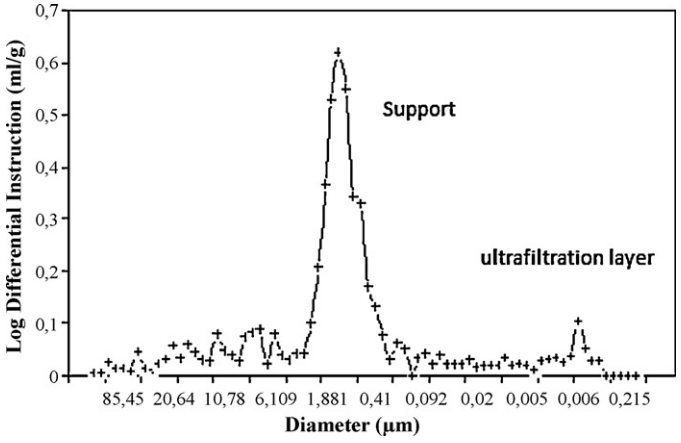


Fig. 14. Pore diameters of zirconia ultrafiltration layer.

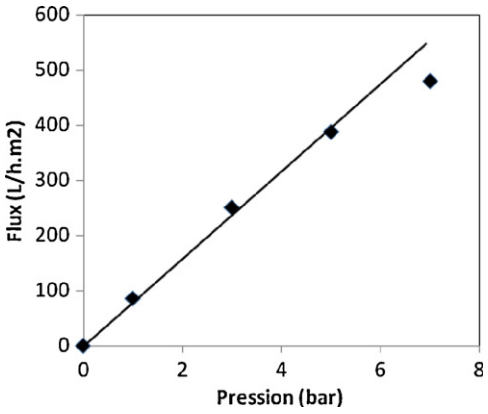


Fig. 15. Water flux permeability versus working pressure.

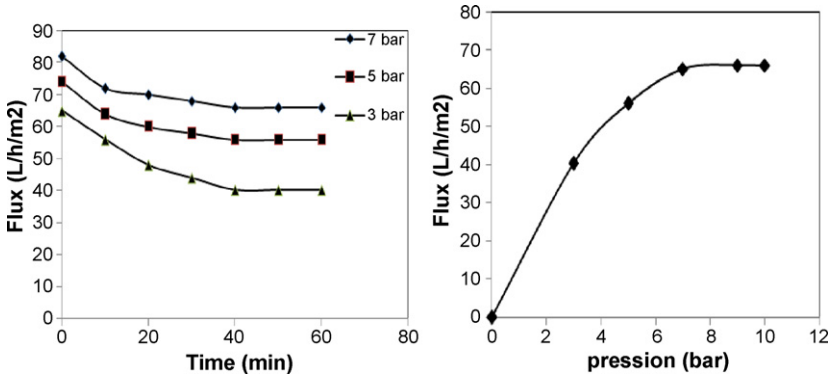


Fig. 16. Variation of permeate flux with the time and pressure.

Table 3a
Characteristics of the effluent before and after filtration using prepared UF membrane.

| Sample | Conductivity (mS/cm) | Turbidity (NTU) | TRCOD (%) |
|---|---|---|---|
| Raw effluent | 81.5 | 1300 | – |
| Permeate ($P$ = 3 bar) | 67.6 | 1.25 | 60 |
| Permeate ($P$ = 5 bar) | 69.3 | 1.38 | 65 |
| Permeate ($P$ = 7 bar) | 70.1 | 1.40 | 67 |

Table 3b
Characteristics of the effluent before and after ultrafiltration at 3 bar using commercial and elaborated membranes.

| Sample | Conductivity (mS/cm) | Turbidity (NTU) | TRCOD (%) |
|---|---|---|---|
| Raw effluent | 81.5 | 1300 | – |
| Permeate from elaborated UF membrane | 67.6 | 1.25 | 60 |
| Permeate from commercial UF membrane | 72 | 1.45 | 70 |

## 4. Application to the treatment of the cuttlefish effluents

Membrane processes can be used for the treatment of the wastewater coming from the sea product conditioning [17]. Thus, the elaborated ultrafiltration membranes have been applied to the cuttlefish effluents treatment produced from cuttlefish conditioning and freezing process which represents an activity widely used in Sfax. Samples were collected from a sea product-freezing factory located in Sfax (Tunisia). The dark colour in this effluent was due to the presence of sepia ink as suspension particles which have a size range between 56 and 161 nm [18].

Fig. 16 gives the variation of permeate flux with transmembrane pressure. Permeate flux increased linearly with transmembrane pressure until 7 bar and then became pressure independent. This behaviour can be explained by the formation of a concentrated polarization layer. Beyond 7 bar, the flux value is about 66 l/h m$^2$.

Table 3a gives the main characteristics of the raw and treated effluent. It can be observed that the turbidity (Turbidimeter HACH RATIO 2100A) of the permeate was very low (inferior to 1.5 NTU) and that the COD retention rate determined at 3 bar (COD is Chemical Oxygen Demand determined by colorimetric method) exceeded 60%. The initial COD of the raw effluent is about 2600 mg/l. However, the conductivity in the permeate decreases slightly and is pressure independent. These results confirm the efficiency of the UF prepared membranes to cuttlefish conditioning effluent clarification.

The UF prepared membrane performances are compared with those achieved by Alumina commercial UF membrane having a weight cut off of 300 kDa.

Table 3b shows that UF performances are similar with the two UF membranes: prepared membrane zirconium/mud of hydrocyclone laundries of phosphate and commercial alumina/alumina membrane.

## 5. Conclusion

In this work we have developed a low cost membrane support using a subproduct coming from the phosphate industry transformation. The support was prepared by extrusion of the mud of hydrocyclone laundries of phosphate after crushing. The mechanical and structural properties of the support are satisfying in terms of porosity and pore diameter. The obtained ceramic support sintered at 900 °C has a mean pore diameter of about 1.05 μm with an average porosity of 39%. The composite ultrafiltration membrane based on zirconium/mud of hydrocyclone laundries of phosphate has a water permeability of 86 l/h m$^2$ bar.

The application of this membrane to the washing cuttlefish effluent treatment shows good performances in term of permeate flux and pollution retention. The results were similar to those obtained using commercial ultrafiltration alumina membrane.

## List of symbols

| | |
|---|---|
| $P_{inlet}$ | inlet pressure (bar) |
| $P_{outlet}$ | outlet pressure (bar) |
| $P_f$ | filtrate pressure (bar) |
| $J_w$ | water flux (l/h m$^2$) |
| $L_p$ | water permeability (l/h m$^2$ bar) |

## References

[1] S.H. Lee, K.C. Chung, M.C. Shin, J.I. Dong, H.S. Lee, K.H. Auh, Preparation of ceramic membrane and application to the cross flow microfiltration of soluble waste oil, Mater. Lett. 52 (2002) 266–271.

[2] C. Gaucher, P. Jaouen, J. Comiti, P. Legentilhomme, Determination of cake thickness and porosity during cross-flow ultrafiltration on a plane ceramic membrane surface using an electrochemical method, J. Membr. Sci. 210 (2002) 245–258.
[3] T.V. Gestel, C. Vandecasteele, A. Buekenhoudt, C. Dotremont, J. Luyten, R. Leysen, et al., Alumina and titania multilayer membranes for nanofiltration: preparation, characterization and chemical stability, J. Membr. Sci. 207 (2002) 73–89.
[4] R.F.S. Lenza, W.L. Vasconcelos, Synthesis and properties of microporous sol–gel silica membranes, J. Non-Cryst. Solids 273 (2000) 164.
[5] G.E. Romanos, Th. Steriotis, A. Kikkinides, E.S. Kanellopoulos, N.K. Kasseelouri, J.D.F. Ramsay, P. Langlois, S. Kallus, Innovative methods for preparation and testing of $Al_2O_3$ supported silicalite-l membranes, J. Eur. Ceram. Soc. 21 (2001) 119–126.
[6] S. Khemakhem, A. Larbot, R. Ben Amar, New ceramic microfiltration membranes from Tunisian natural materials: application for the cuttlefish effluents treatment, Ceram. Int. 35 (2009) 55–61.
[7] S. Masmoudi, A. Larbot, H. El Feki, R. Ben Amar, Elaboration and characterisation of apatite based mineral supports for microfiltration and ultrafiltration membranes, Ceram. Int. 33 (2007) 337–344.
[8] I. Jedidi, S. Khemakhem, A. Larbot, R. Ben Amar, Elaboration and characterisation of fly ash based mineral supports for microfiltration and ultrafiltration membranes, Ceram. Int. 35 (2009) 2747–2753.
[9] I. Khiari, I. Chaari, E. Fakhfakh, M. Medhioub, F. Jamoussi, Les Premières Journées Tunisiennes sur la Valorisation des Argiles, Borj Cédria, 2010 May 25.
[10] I. Jedidi, S. Saïdi, S. Khemakhem, A. Larbot, N. Elloumi-Ammar, A. Fourati, A. Charfic, A. Ben Salah, R. Ben Amar, Elaboration of new ceramic microfiltration membranes from mineral coal fly ash applied to waste water treatment, J. Hazard. Mater. 172 (2009) 152–158.
[11] Y.-F. Hsu, S.-F. Wang, Y.-R. Wang, S.-C. Chen, Effect of niobium doping on the densification and grain growth in alumina, Ceram. Int. 34 (2008) 1183–1187.
[12] F. Bouzerara, A. harrabi, S. Achour, A. Larbot, Pourous ceramic supports for membranes preparead from kaolin Doloma mixtures, J. Eur. Ceram. Soc. 26 (2006) 1663–1671.
[13] K. Kandori, N. horigami, A. Yasukawa, T. Ishikawa, J. Am. Ceram. Soc. 80 (1997) 1157.
[14] S.J. Joris, C.H. Amberg, J. Phys. Chem. 75 (1971) 3172.
[15] B.O. Fowler, Infrared spectra of apatite, in: W.E. Brown, R.A. Young (Eds.), International Symposium on Structural Properties of Hydroxyapatite and Related Compounds, Gaithersburg, MD, 1968 (Chapter 7).
[16] L.R. Zapanta, Nature 403 (1965) 206.
[17] D.W. Halcomb, R.A. Young (Eds.), Thermal decomposition of human tooth enamel and calcif, Tissue Int. 31 (1980) 189.
[18] S. Khemakhem, Elaboration de membranes de microfiltration et d'ultrafiltration en céramique a‘ base d'argile tunisienne, PhD thesis, Université de Sfax, Tunisia, 2005.
[19] S. Masmoudi, Elaboration de membranes de microfiltration et d'ultrafiltration en céramique a‘ base de phosphate tunisien, PhD thesis, Université de Sfax, Tunisia, 2005.